ELSEVIER

Polymer 43 (2002) 6641–6651

polymer

www.elsevier.com/locate/polymer

Core-corona nanoparticles formed by high molecular weight poly(ethylene oxide)-*b*-poly(alkylglycidyl ether) diblock copolymers

P. Petrov[a], S. Rangelov[a,b], Ch. Novakov[a], W. Brown[b], I. Berlinova[a], Ch.B. Tsvetanov[a,*]

[a]*Institute of Polymers, Bulgarian Academy of Sciences, 1113 Sofia, Bulgaria*
[b]*Department of Physical Chemistry, University of Uppsala, P.O. Box 532, 75121 Uppsala, Sweden*

Received 7 June 2002; received in revised form 11 September 2002; accepted 12 September 2002

Abstract

Novel high molecular weight poly(ethylene oxide)-*b*-poly(alkylglycidyl ether) diblock copolymers have been synthesized by sequential anionic-coordination polymerization using a calcium amide–alkoxide initiating system. The hydrophobic blocks were formed by polymerization of alkylglycidyl ethers differing in the size of the hydrophobe and the length of the oxyethylene spacer between the terminal hydrophobes and the polymerizable epoxy group. The length of the spacer was 0, 2 or 10 oxyethylene units. The content of the hydrophobic groups in the copolymers was about 2 wt% as determined by ^{1}H NMR and the molecular weights were found to be up to 1.8×10^6 g/mol by using GPC and SLS. The aqueous solution properties of the copolymers were studied by static fluorescence, static and dynamic light scattering and transmission electron microscopy. The copolymers were found to self-associate in core-corona type particles in a relatively narrow concentration range. The aggregation numbers and the dimensions of the aggregates were determined by a combination of dynamic and static light scattering molecular weights. Core-corona nanoparticles of low aggregation number (3–5) and slightly extended coronae were found to coexist with unassociated macromolecules in the concentration range between the critical aggregation concentration and the overlap concentration. Both particles were visualized by TEM. © 2002 Elsevier Science Ltd. All rights reserved.

Keywords: Polymeric nanoparticles; Block copolymers; Poly(ethylene oxide)

1. Introduction

Polymeric nanoparticles have attracted a rapidly growing interest. Numerous applications such as drug delivery [1–5], nanoreactors [5–7], separation technologies [5,8], clinical diagnostics [1,9], etc. emanate from their unique size-associated properties, namely, large specific surface area, compact structure, defined shape. In the last decades serious attempts have been made to develop amphiphilic block and graft copolymers that are able to form core-corona nanoparticles with prescribed morphologies and physical properties in selective solvents. The anisotropic interactions between the solvent molecules and the copolymer chains have been shown to be the driving force for the micellization process. Thus, the solvent-insoluble segments form a compact micellar core and the solvent-soluble segments form a micellar corona. The corona prevents the progressive aggregation of the core and stabilizes the micelles.

Much of the literature on self-assembly of amphiphilic copolymers in selective solvents describes the behavior of hydrophilic/hydrophobic copolymers in aqueous media. Poly(ethylene oxide) (PEO) (commonly referred to as polyethylene glycol or PEG) is most frequently used as a hydrophilic corona-forming block. PEO is well soluble and highly hydrated in water, and shows a large exclusion volume, which favors the steric repulsion. Its steric stabilization ability together with other PEO properties such as biocompatibility, non-toxicity, non-immunogenicity, protein resistance, high solubility in many organic solvents, make PEO the most favored corona-forming polymer. Amphiphilic copolymers of molecular weights usually below 100 kDa with PEO block molecular weights ranging from 1 to 15 kDa have been extensively studied. However, there is still a dearth of information concerning the behavior of high molecular weight PEO-based hydrophilic/hydrophobic copolymers. It has been shown previously [10] that PEO chains of up to 6.0×10^5 molecular

* Corresponding author. Tel.: +359-2-700-138; fax: +359-2-707523.
E-mail address: chtsvet@polymer.bas.bg (C.B. Tsvetanov).

0032-3861/02/$ - see front matter © 2002 Elsevier Science Ltd. All rights reserved.
PII: S0032-3861(02)00645-6

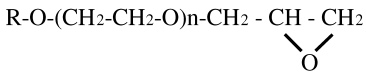

Scheme 1.

weight follow the expected patterns of behavior for a flexible chain in a good solvent. However, PEO chains of higher molecular weights undergo microgel formation and collapse to a more compact structure, which is probably stabilized by intramolecular hydrogen bonding mediated through water molecules. Such interactions are also expected to take place in the coronae of aggregates formed by high molecular weight PEO-based amphiphiles. This would result in formation of coronae that markedly differ from the coronae formed by the conventional amphiphilic copolymers of much lower molecular weights. In contrast to the latter, the former coronae could be considered as a single separate entity, in which both the repulsive forces between the chains and the unimer exchange are greatly diminished, thus affecting the aggregate stability.

The present work was motivated by the strong interest of the industry in high molecular weight PEO-based materials [11–13] and the self-assembly of amphiphilic copolymers [14–19]. Here we report on the synthesis and the characterization of novel high molecular weight poly(ethylene oxide)-*b*-poly(alkylglycidyl ether) diblock copolymers. The hydrophobic blocks of these amphiphilic copolymers are constructed by polymerization of epoxide monomers with the structure shown in Scheme 1.

As seen, the hydrophobic moiety (dodecyl/tetradecyl or octadecyl) is separated from the epoxy group by a flexible spacer of various length. The copolymers were obtained by using an initiating system, developed for the industrial production of high molecular weight PEO [20,21].

2. Experimental

2.1. Materials

Brij®72 and Brij®76 (Aldrich), ethylene oxide (Clariant), dodecyl/tetradecyl glycidyl ether (Aldrich), and epibromohydrin (Aldrich) were used as received. All solvents were purified by standard procedures.

2.2. Synthesis

2.2.1. Monomers

Brij72-glycidyl ether and Brij76-glycidyl ether were synthesized according to the following procedure: Brij®72 ($M_w \sim 359$ g/mol) or Brij®76 ($M_w \sim 711$ g/mol) 0.014 M was dissolved in toluene and dried by azeotropic distillation. Thereafter, Brij® was dissolved in 150 ml of dry tetrahydrofuran and treated with sodium hydride (0.021 mol) at 30 °C for 4 h under nitrogen atmosphere to metallize the terminal hydroxyl group. Epoxidation was achieved by adding epibromohydrin (0.056 mol) to the solution. The reaction mixture was stirred at 40 °C for additional 6 h and then precipitated in anhydrous ether. The ether solution was decanted; the residue was washed several times with ether and dried to constant weight. Methylene chloride was added to dissolve the product (Brij72-epoxide or Brij76-epoxide) and the insoluble NaBr was separated by centrifugation and filtration. Finally, the transparent solutions of Brij-epoxides were precipitated again in anhydrous ether. The solvent was removed and pale yellow products (yield ~ 75 wt%) were obtained. The monomers were dried in vacuum at 10^{-3} mm Hg and their purity was checked by ^{1}H NMR. The ^{1}H NMR spectrum of Brij®72 and Brij®76 in DMSO-d_6 shows a resonance for the hydroxyl group as a sharp triplet at 4.58 ppm. This resonance is absent in the ^{1}H NMR spectrum of Brij72-epoxide and Brij76-epoxide in the same solvent. The degree of end group modification was determined from the spectrum of Brij72(76)-epoxide in $CDCl_3$ by comparing the area of the epoxy group peaks at 3.16, 2.79 and 2.6 ppm to that of the methyl group signal at 0.88 ppm (Fig. 1).

2.2.2. Preparation of the initiating system

The preparation of the calcium amide–alkoxide initiating system, described in detail elsewhere [20], includes the following steps. The initiating system was prepared directly in the reaction vessel, equipped with a mechanical stirrer and an argon line. 70 cm^3 of ammonia, 15 cm^3 of heptane, and 1.3 cm^3 of EO were placed in a dry precooled 1 l four-necked flask and stirred. Then, 1 g of calcium metal was added. After dissolving the Ca, the liquid ammonia was evaporated by gentle heating to room temperature. Finally, 85 cm^3 of heptane were added to the slurry and the mixture was refluxed for 1 h.

2.2.3. Copolymerization

Diblock copolymers having pendant hydrophobic aliphatic groups were synthesized by sequential, anionic-coordination polymerization of the hydrophobic monomer (D/TGE, Brij72GE or Brij76GE) and ethylene oxide (EO) at 97 and 40 °C, respectively. A typical run followed: 2 g of hydrophobic monomer were added to the suspension of the catalyst. The mixture was refluxed for 2 h. Then the temperature was decreased to 40 °C and EO was bubbled through the reaction mixture for 8 h. Portions of 100 cm^3 of heptane were added during the polymerization to assure effective agitation of the resulting dispersion. The copolymer precipitate obtained was separated by filtration, thoroughly washed with hexane and dried.

2.2.4. Copolymer purification

An extraction with anhydrous ethanol at 15 °C was performed to remove a possible hydrophobic homopolymer as well as the ethanol soluble low-molecular weight fractions.

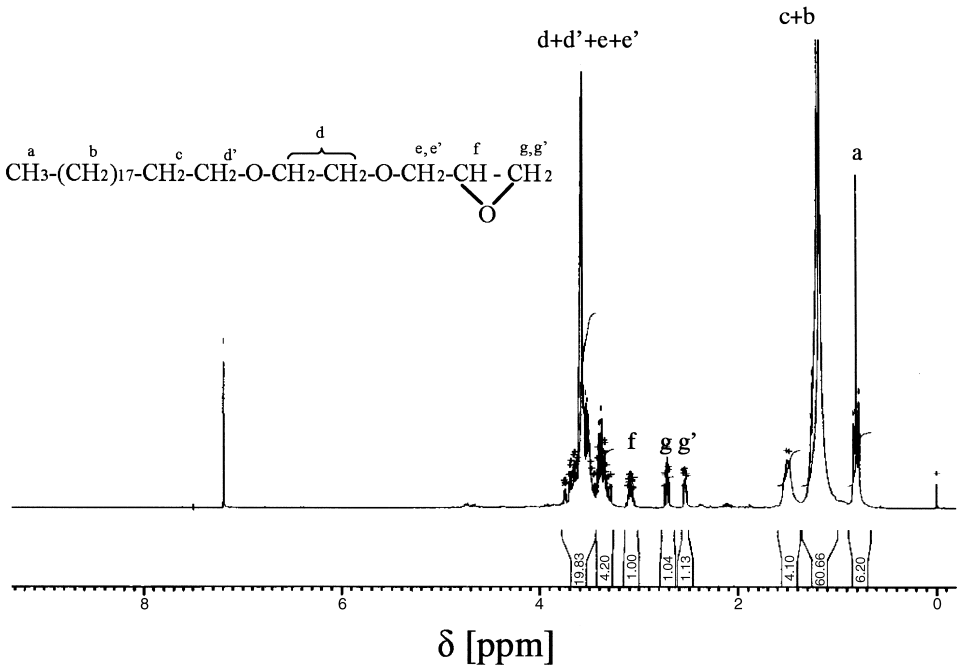

Fig. 1. ^{1}H NMR spectrum of Brij72-epoxide in chloroform.

The Ca residue was removed by the following procedure: aqueous solution of citric acid (0.01 wt%) was added dropwise to the copolymer aqueous solution (0.5 wt%) while stirring until pH 7. The Ca-citrate obtained was separated from the copolymer by dialysis against distilled water with a cellulose membrane (D-9527, Sigma; cut-of value of 12,000 g/mol).

2.2.5. Preparation of core-corona nanoparticles

Polymeric nanoparticles were formed by the solvent exchange (nanoprecipitation) method [22]. The copolymer sample (0.2 g) was dissolved in acetone (10 cm^3), filtered through 0.45 μm pore size filters, and then the solution was added to 100 cm^3 of prewarmed (60 °C) distilled water under stirring. Thus the organic solvent was evaporated, and then the nanoparticles formed were lyophilized.

2.3. Methods

2.3.1. NMR-spectroscopy

^{1}H NMR-spectra of ~2 wt% solutions in $CDCl_3$ or DMSO-d_6 were recorded on a Bruker WM250 spectrometer operating at 250 MHz. The copolymer compositions were determined from the proton signals characteristic for the methylene groups in the aliphatic chain units ($\delta = 1.25$ ppm) and in the EO chain units ($\delta = 3.55$ ppm), respectively.

2.3.2. Gel permeation chromatography

Copolymer molecular weights and molecular weight distributions were studied by GPC. The analyses were performed with 0.5 wt% LiBr in dimethylacetamide at 70 °C as an eluent at a flow rate 1 cm^3/min; 100 μl of about 0.15 wt% polymer solutions were injected. The column sets employed were 300 × 8 mm, 10 μm PSS-GRAM: 30, 30, 100, and 3000 Å. The system was calibrated with polystyrene standards of known molecular weight.

2.3.3. Fluorescence measurements

Fluorescence spectra, with the fluorescent probe pyrene, were recorded on a SPEX-fluorolog 1650 0.22-m double spectrometer (SPEX Industries Inc., Edison, NJ). The emission measurements were performed between 350 and 450 nm with an excitation wavelength at 320 nm. Slitwidths were set to 1 mm and the temperature was controlled by means of water jacketed cuvette holder connected to a thermostat.

Appropriate volumes of a stock solution of pyrene in ethanol were transferred into a number of cylindrical vials. The solvent was removed under a stream of nitrogen and thereafter under vacuum for 24 h. Suitable amounts of stock solutions of the copolymers and purified water (Millipore Super-Q-System) filtered through 0.45 μm pore size filters were added to the vials to give a final volume of 2 cm^3 and a final pyrene concentration of 5×10^{-7} M. The samples were incubated in the dark for 24 h at room temperature. The measurements were done at 25 °C.

2.3.4. Light scattering

The light scattering setup consists, as described previously [17], of a 488 nm Ar ion laser and the detector optics with an ITT FW 130 photomultiplier and ALV-PM-PD amplifier-discriminator connected to an ALV-5000 autocorrelator built into a computer. Measurements were made at different angles in the range of 50–130° and at different concentrations and at 25 °C. Information on the molecular

weight (M_w), the radius of gyration (R_g), and the second virial coefficient (A_2) was obtained from the dependence of the reduced scattered intensity Kc/R_Θ on the concentration (c) and the scattering angle (Θ) measured in the simultaneous static and dynamic experiments. Here $K = (4\pi^2 n^2/N_A\lambda^4)(dn/dc)^2$, N_A is Avogadro's constant and λ the wavelength. With large particles, when $qR_g < 1$, the reduced scattered intensity is angle-dependent and R_g is determined from the ratio of the initial slope to intercept of such plots for the data extrapolated to zero concentration. Similarly, A_2 is derived from the slope of the zero angle data. The refractive index increment (dn/dc) was measured in a differential refractometer with Rayleigh optics. For the present copolymers, dn/dc of 0.131, 0.141 and 0.142 cm^3/g for copolymers PEO-D/TGE, PEO-Brij72GE, and PEO-Brij76GE, respectively, were obtained at the wavelength used and 25 °C. The Rayleigh ratio was determined as $R_\Theta = [(I - I_0)/I_{ref}]R_{ref}(n/n_{ref})^2$. Here $n = 1.33$ is the solvent refractive index and n_{ref} that of toluene. I is the measured total time-averaged scattered intensity, I_0 that of the solvent, water, and I_{ref} that of toluene. Toluene was used as the reference scatterer ($R_{ref} = 4.0 \times 10^{-7}$ m^{-1} at $\lambda = 488$ nm).

Analysis of the dynamic data was performed by fitting the experimentally measured $g_2(t)$, the normalized intensity autocorrelation function, which is related to the electrical field correlation function $g_1(t)$ by the Siegert relationship [18]:

$$g_2(t) - 1 = \beta|g_1(t)|^2 \quad (1)$$

where β is a factor accounting for deviation from ideal correlation. For polydisperse samples, g_1(t) can be written as the inverse Laplace transform (ILT) of the relaxation time distribution, $\tau A(\tau)$

$$g_1(t) = \int \tau A(\tau)\exp(-t/\tau)\mathrm{d}\ln\tau \quad (2)$$

where t is the lag-time. The relaxation time distribution, $\tau A(\tau)$, is obtained by performing ILT using the constrained regularization algorithm REPES [19]. A mean diffusion coefficient D is calculated from the second moment of each peak as $D = \Gamma/q^2$, where q is the magnitude of the scattering vector $q = (4\pi n/\lambda)\sin(\Theta/2)$ and $\Gamma = 1/\tau$ is the relaxation rate of each mode.

Within the dilute regime, D varies linearly with the concentration according to

$$D = D_0(1 + k_D C + \cdots) \quad (3)$$

where D_0 is the diffusion coefficient at infinite dilution and k_D is the hydrodynamic 'virial' coefficient. The Stokes–Einstein equation relates D_0 to the hydrodynamic radius (R_h):

$$R_h = kT/(6\pi\eta D_0) \quad (4)$$

kT is the thermal energy factor and η is the temperature-dependent viscosity of the solvent.

2.3.5. Transmission electron microscopy

The morphology of the nanoparticles was observed on a transmission electron microscope (JEOL 100B). A drop of the nanoparticles suspension in aqueous medium was placed on a carbon film coated on a copper grid for TEM and freeze-dried. The observations were done at 80 kV.

3. Results and discussion

3.1. Synthesis of the diblock copolymers

The calcium amide–alkoxide initiating system has been developed for the production of commercial HMW PEO [20,21]. We used this initiating system to prepare HMW poly(ethylene oxide)-*b*-poly(alkylglycidyl ether) diblock copolymers. The copolymers were synthesized via sequential suspension polymerization of the monomer, forming the hydrophobic block (D/TGE, Brij72GE or Brij76GE), and EO following an anionic-coordination mechanism. The homopolymerization of hydrophobically modified glycidyl ethers proceeded only at elevated temperatures. The monomers polymerized in heptane almost quantitative at reflux, while at 40 °C, the conversion was negligible. The results suggested that in two-stage process when hydrophobic glycidyl ether was polymerized at reflux and then EO was copolymerized at 40 °C, the second block was practically pure PEO. To obtain different chain structure, the type of the first monomer was varied. These three monomers were chosen as to compare their behavior due to the presence of an oxyethylene spacer in their molecules as well as the effect of the size of the spacer (Scheme 1). It has been reported that a small difference in the oxyethylene chain length in $R(EO)_nOH$ strongly affects the formation of micelles in aqueous solution [23]. Therefore, copolymers with EO spacers of different length between the polymer backbone and the hydrophobic chains were obtained by synthesizing two novel monomers: $C_{18}H_{37}(EO)_2$-glycidyl ether (Brij72GE) and $C_{18}H_{37}(EO)_{10}$-glycidyl ether (Brij76GE).

After purification, the copolymers were characterized by ^{1}H NMR and GPC. From the peak area ratio of the methylene protons of the EO units and that of the aliphatic groups, located at 3.55 and 1.25 ppm, respectively, a weight content of the aliphatic hydrophobic groups was calculated (Table 1).

The GPC analyses showed copolymers with high molecular weight ($M_w = 0.8–1.3 \times 10^6$). The molecular weight distributions of the copolymers were unimodal, whereas the M_w/M_n values were relatively high (4.9–8.4) since the polymerizations with the calcium-based initiating system were heterogeneous precipitation polymerizations (Table 1).

Table 1
Characterization of poly(ethylene oxide)-*b*-poly(alkylglycidyl ether) diblock copolymers

Copolymer	Hydrophobic groups content (wt%)[a]	$10^{-6} \times M_n$ (g/mol)[b]	$10^{-6} \times M_w$ (g/mol)[b]	M_w/M_n
PEO-D/TGE	1.5	0.15	0.75	4.9
PEO-Brij72GE	1.2	0.13	0.92	6.9
PEO-Brij76GE	2.3	0.16	1.34	8.4

[a] Calculated by ^{1}H NMR.
[b] Measured by GPC.

3.2. Fluorescent measurements

The aggregation behavior of the copolymers was investigated by fluorescence using pyrene as a probe. The ratio between the intensities of the first and third peak in the pyrene emission spectrum (I/III), is known to depend on the polarity of the environment [24]. This property has been widely used to monitor aggregation processes of surfactants or amphiphilic polymers in aqueous solution [18,23–28]. Upon micellization I/III decreases over a rather narrow concentration range as shown for conventional surfactants, SDS and $C_{12}(EO)_6$ [18]. In contrast, the I/III transition for amphiphilic polymers occurs over a much broader concentration interval, reaching sometimes orders of magnitudes [18,19,29]. Fig. 2 shows the variation of I/III with the concentration of the copolymers PEO-D/TGE, PEO-Brij72GE, PEO-Brij76GE. At low concentration I/III is about 1.60.

A value of 1.62 was obtained for pyrene in pure water. This indicates that pyrene molecules are mainly in the aqueous phase and that there are no hydrophobic domains in the solution. At a given polymer concentration the curves show an abrupt decrease of I/III. The process is considered to be complete when the low plateau of the I/III value is reached. At these copolymer concentrations all of the pyrene is present in a hydrophobic environment, which implies that hydrophobic domains are formed. As seen from Fig. 2, the aggregation process for the three copolymers occurs roughly in the same concentration range (2.5×10^{-4}–7.2×10^{-3} g/cm^3). Surprisingly, the transition is not as broad as expected for molecules of such large dimensions and wide molecular weight distribution. It occurs over less than an order of magnitude, being somewhat narrower for the copolymer PEO-Brij76GE. This unusual feature can be attributed to the flexible spacer, which is incorporated between the hydrophobic group and the copolymer main chain. The spacer serves to decouple the different motions and gives the hydrophobic group more freedom of movement. The enhanced mobility of the hydrophobic groups makes the transition narrower. The critical aggregation concentrations of 1.0×10^{-3}, 1.1×10^{-3}, and 1.2×10^{-3} g/ml, for copolymers PEO-D/TGE, PEO-Brij72GE, and PEO-Brij76GE, respectively, were determined as inflection points in the I/III vs. *C* curves.

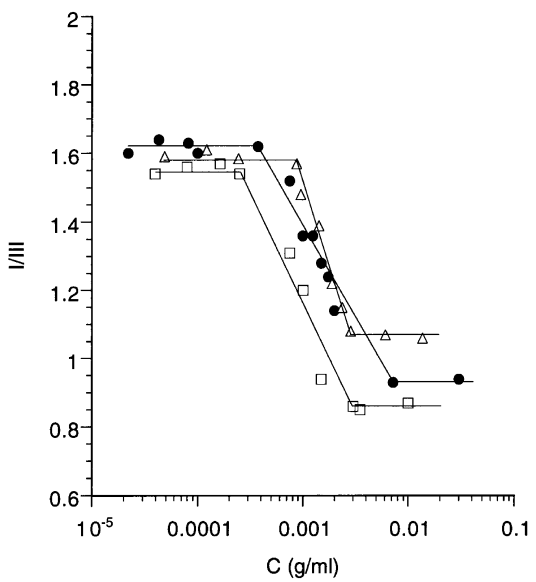

Fig. 2. Variation of the intensity ratio I/III of the fluorescence spectrum of pyrene in aqueous solutions of copolymers PEO-Brij72GE (●), PEO-D/TGE (□), and PEO-Brij76GE (△) at 25 °C.

3.3. Light scattering measurements

3.3.1. Low concentrations, $C < CAC$

Static and dynamic light scattering experiments were carried out simultaneously in the concentration range of 0.7–9.0×10^{-4} g/ml. This concentration range was below the CAC region as determined by fluorescence measurements and single coil behavior was expected. However, clustering that derives from intermolecular hydrogen bonding involving the ether oxygens, together with the intrinsically broad molecular weight distribution, frequently complicates the interpretation of the solution properties of PEO-based polymers. The effectiveness of small pore size filters in eliminating non-micellar aggregates from solutions of high molecular weight samples has been demonstrated earlier by a number of authors [10,30,31].

Fig. 3 shows an example of an autocorrelation function and the corresponding relaxation time distribution for copolymer PEO-Brij72GE. The distributions were bimodal containing a low intensity fast mode that corresponded to less than 10% of the scattered intensity at 90°. As concluded for the high molecular weight homo PEO [10], the non-diffusive fast mode was found to derive in part from internal

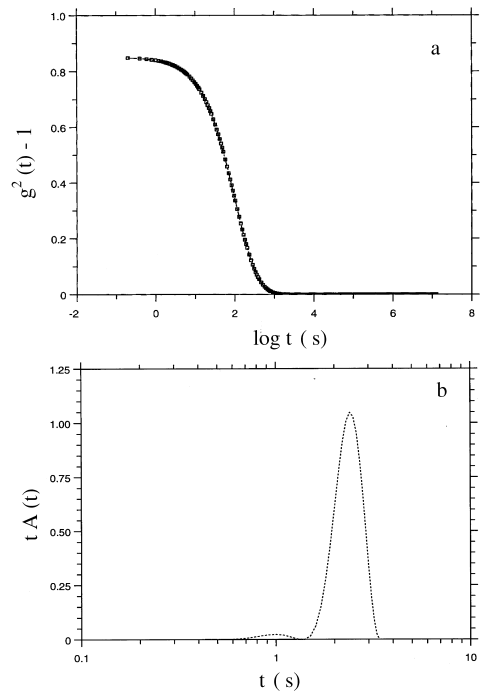

Fig. 3. (a) Autocorrelation function for the copolymer PEO-Brij72GE at $c = 7.15 \times 10^{-4}$ g/ml, angle 90° and 25 °C. (b) Corresponding relaxation time distribution data in (a).

modes and was thus of marginal interest as far as the determination of the molecular weight is concerned.

The dominant peaks were shown to be diffusive from the linear dependence of the relaxation rate, Γ, on $\sin^2(\Theta/2)$ (Fig. 4); the diffusion coefficients were determined as slopes of the linear fit and then plotted against concentration, and extrapolated to zero concentration (Fig. 5).

The intercept gives the diffusion coefficients, D_0, which were used to calculate the hydrodynamic radii, R_h (Eq. (5)).

Table 2
Static and dynamic light scattering characterization data for the copolymers in the low concentration range, $C <$ CAC

Copolymer	$10^{-6} \times M_w$ (g/mol)	$10^3 \times A_2$ (mol ml/g^2)	R_g (nm)	$10^{12} \times D_0$ (m^2/s)	R_h (nm)
PEO-D/TGE	1.78	2.08	70.9	4.57	53.6
PEO-Brij72GE	0.67	0.89	58.1	8.47	28.7
PEO-Brij76GE	0.71	2.76	55.9	6.85	32.1

M_w, weight-average molecular weight; A_2, second virial coefficient; R_g, radii of gyration; D_0, diffusion coefficient at infinite dilution; R_h, hydrodynamic radius.

D_0 and R_h are summarized in Table 2. It may be noted that the concentration dependence of the diffusion coefficients was weak (Fig. 5), i.e. they were slightly affected by interparticle interactions.

The weight-average molecular weights (M_w), radii of gyration (R_g) and second virial coefficients (A_2) were determined from SLS experiments by constructing Zimm plots. Fig. 6 shows a typical Zimm plot for copolymer PEO-Brij72GE.

The parameters evaluated from the SLS experiments are listed in Table 2. The weight-average molecular weights varied from 0.67×10^6 to 1.78×10^6 g/mol. The second virial coefficients were invariably positive indicating favorable particle-solvent interactions. They were of the same order of magnitude as the second virial coefficients for HMW homo PEO [10], implying that in the low-concentration range A_2 is not significantly influenced by the incorporation of hydrophobic groups into the copolymer macromolecule.

The magnitudes of R_g and R_h were also generally greater compared to those of other linear flexible polymer chains in good solvents [32,33]. The power law fit between R_h and

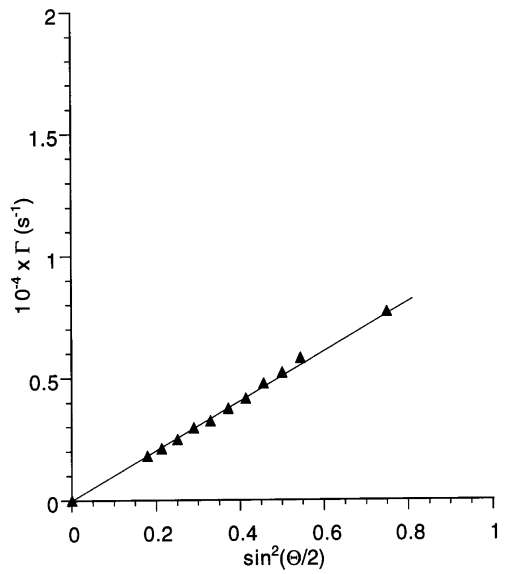

Fig. 4. Relaxation rate (Γ) of the dominant mode as a function of $\sin^2(\Theta/2)$ for a 7.15×10^{-4} g/ml solution of the copolymer PEO-Brij72GE.

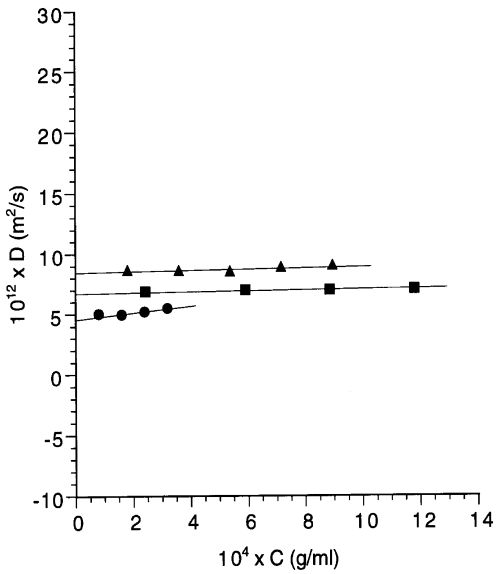

Fig. 5. Concentration dependence of diffusion coefficients for copolymers PEO-Brij72GE (▲), PEO-D/TGE (●), PEO-Brij76GE (■).

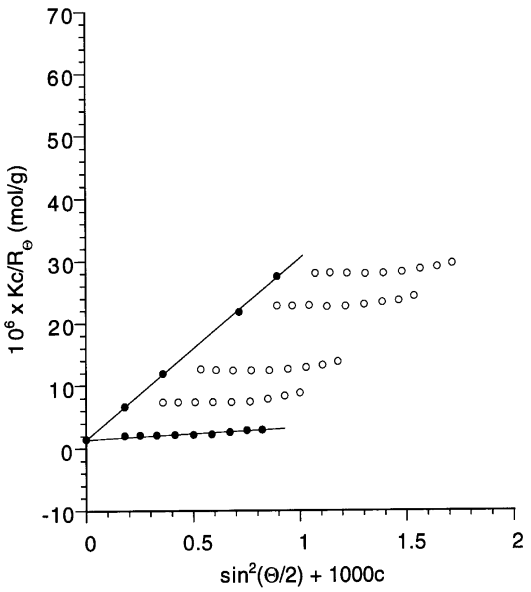

Fig. 6. Zimm plot of the copolymer PEO-Brij72GE in the concentration range below CAC. Experimental points (open symbols), extrapolated points to zero concentration and zero scattering angle (filled symbols).

molecular weight given by the empirical relationship of Devanand and Selser [33] established for unmodified PEO in water (Eq. (5))

$$R_h(\text{nm}) = 0.0145 M_w^{0.571} \quad (5)$$

gives values of 30.8, 54.0, and 31.8 nm for PEO-Brij72GE, PEO-D/TGE, and PEO-Brij76GE, respectively. These values are in excellent agreement with the experimentally observed hydrodynamic radii (Table 2).

Power law behavior for the radii of gyration was observed for copolymers PEO-Brij72GE and PEO-Brij76GE. The experimentally observed values were close to those deduced from the empirical law of Devanand and Selser for R_g [33] (Eq. (6)).

$$R_g(\text{nm}) = 0.0215 M_w^{0.583} \quad (6)$$

A deviation of R_g from the expected power law (Eq. (6)) was observed for the copolymer of highest molecular weight, PEO-D/TGE; the experimental value of 70.9 nm was lower than the calculated one from Eq. (6) (94.6 nm). This yields the value $R_g/R_h = 1.32$ in contrast to the typical value of 1.8 for highly swollen polymer coils [10,33,34]. Such behavior has been observed earlier for a series of HMW homo PEO [10] and is consistent with the chain collapsing to a more compact coil conformation, stabilized by intramolecular hydrogen bonding probably mediated by water molecules.

In summary, the present copolymers follow the pattern of behavior for a flexible chain in a thermodynamically good solvent at a low concentration range. However, the coils are, more extended than is usual for other polymer/good solvent systems. The scaling of R_g and R_h with the molecular weight is similar to that of HMW homo PEO [10]. In this respect the low-concentration range properties of the copolymers are very close to those of the unmodified HMW homo PEO and thus the effect of the hydrophobic groups appears to be negligible.

3.3.2. Intermediate and high concentrations, $C \geq CAC$

As the concentration increases, another diffusive mode appears in the relaxation time spectra. It represents a much slower relaxation process than that corresponding to the dominant peak. The amplitude of the slow mode increases with increasing the concentration. It becomes dominant and reaches a constant amplitude value at concentrations that are close to although lower than the overlap concentration, C^*, determined according to Eq. (7) [35].

$$C^* = 3M_w/4\pi R_g^3 N_A \quad (7)$$

It is important to emphasize that the dramatic changes in the relaxation time distribution occur in the concentration range, in which an abrupt decrease of I/III is observed, thus showing a good correlation between fluorescence and light scattering measurements.

A typical distribution of the relaxation times for the copolymer PEO-D/TGE in the concentration range $CAC < C < C^*$ is presented in Fig. 7.

As seen, the distribution is far from monomodal containing three well-separated peaks. The dependence of the relaxation rates on $\sin^2\Theta/2$ is shown in Fig. 8a and b.

The fastest mode was not found to be linearly dependent on $\sin^2\Theta/2$, i.e. it is non-diffusive (Fig. 8a). In contrast, the intermediate mode is diffusive as evidenced from the linear dependence on $\sin^2\Theta/2$ (Fig. 8a). Its position is slightly displaced from that of the dominant peak in Fig. 2b. It is therefore attributed to unassociated macromolecules, probably homo PEO or macromolecules with a lower content of hydrophobic groups. The slowest mode is also diffusive (Fig. 8b) and is attributed to multichain aggregates. The diffusion coefficients, D_0^{agg}, for the slow mode were determined following routine procedure and the

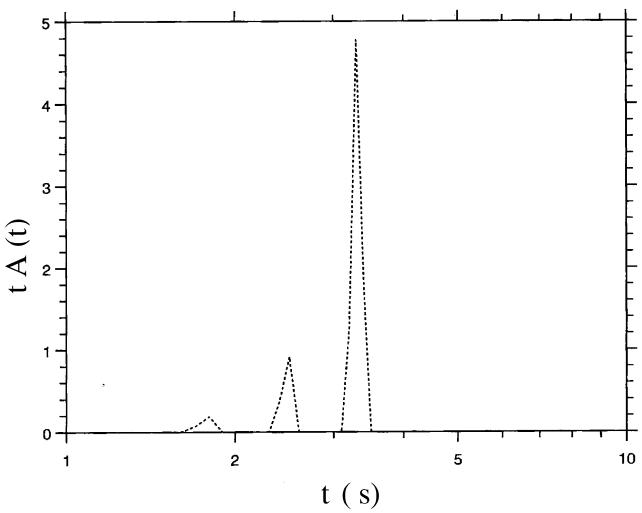

Fig. 7. Spectrum of the relaxation time distribution of 1.33×10^{-3} g/ml aqueous solution of the copolymer PEO-D/TGE.

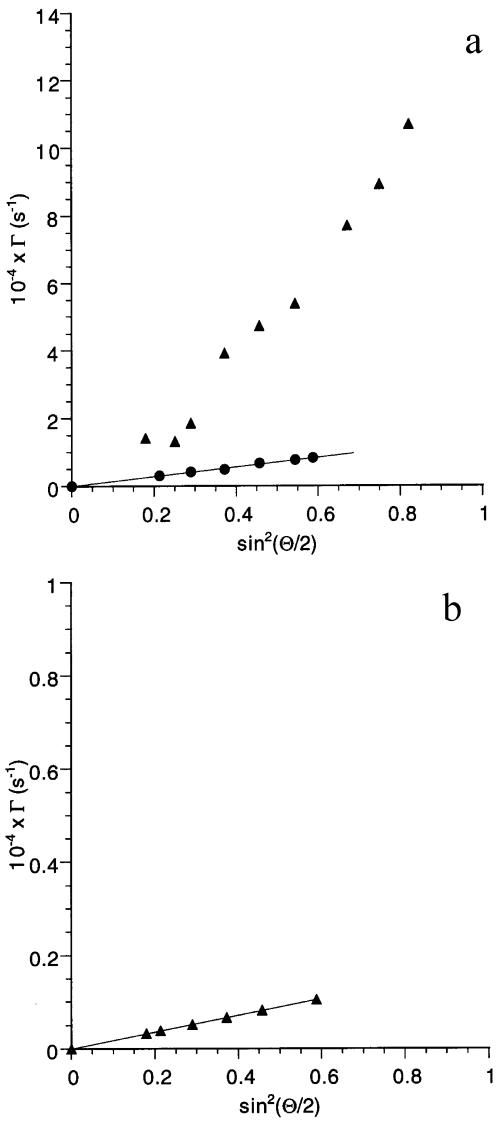

Fig. 8. (a) Relaxation rates of the fast (▲) and intermediate (●) modes as a function of $\sin^2(\Theta/2)$ for a 1.265×10^{-3} g/ml solution of the copolymer PEO-Brij76GE. (b) Relaxation rate of the slow mode as a function of $\sin^2(\Theta/2)$ for the copolymer in (a).

hydrodynamic radii, R_h^{agg}, were calculated using the Stokes–Einstein equation (Eq. (5)). The values of D_0^{agg} and R_h^{agg}, where the superscript agg refers to aggregates, for all copolymers are summarized in Table 3.

Fig. 9 shows a Zimm plot for copolymer PEO-D/TGE, obtained in the concentration range CAC $< C < C^*$.

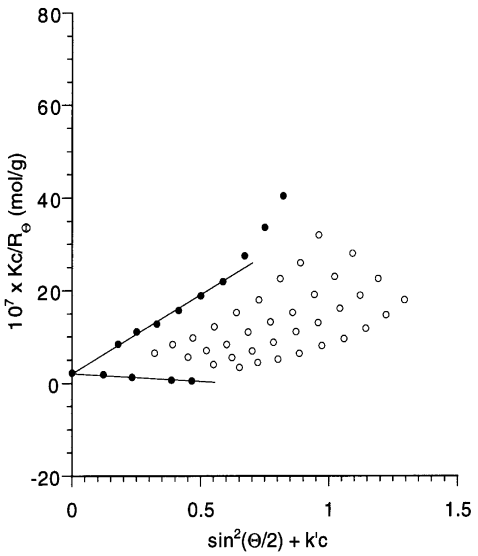

Fig. 9. Zimm plot of the copolymer PEO-D/TGE in the concentration range above CAC. Experimental points (open symbols), extrapolated points to zero concentration and zero scattering angle (filled symbols).

One clear difference between the Zimm plots presented in Figs. 6 and 9 is that the second virial coefficient for these two copolymers changes from positive to negative thus reflecting a change in the solvent/polymer interactions. This finding presumably reflects intermolecular hydrophobic aggregation and is consistent with the appearance of the aggregation peak in DLS. The apparent values of the second virial coefficients, A_2^*, are listed in Table 3. Similarly to PEO-D/TGE, A_2^* for copolymer PEO-Brij72GE changes from positive to negative, whereas copolymer PEO-Brij76GE has a value of A_2^*, which is slightly positive but an order of magnitude lower than A_2, determined in the concentration range well below the CAC (Table 2). The estimated values of the apparent radii of gyration, R_g^*, and the apparent weight-average molecular weight, M_w^*, are listed in Table 3. It should be emphasized that A_2^*, R_g^* and M_w^* contain contributions from both the individual single chains and the multichain aggregates. The second difference is the curvature in the dependence of the reduced scattered intensity on $\sin^2(\Theta/2)$. The non-linearity in the angle-dependence is anticipated when large aggregates are present and the product $qR_g < 1$ may no longer hold at higher angles.

Another aspect of the systems to be considered is the determination of the molecular weight of the aggregates,

Table 3
Static and dynamic light scattering characterization data for the copolymers in the concentration range CAC $< C < C^*$

Copolymer	$10^{12} \times D_0^{agg}$ (m^2/s)	R_h^{agg}(nm)	$10^{-6} \times M_w$ [a] (g/mol)	$10^4 \times A_2$ [a] (mol ml/g^2)	R_g [a] (nm)	X_s	X_{agg}	$10^{-6} \times M_{w,agg}$ (g/mol)	N_{agg}
PEO-D/TGE	0.70	351.7	4.40	−2.07	148.1	0.163	0.837	4.91	2.8
PEO-Brij72GE	1.52	161.5	1.45	−0.97	60.0	0.243	0.757	1.69	2.5
PEO-Brij76GE	1.66	147.7	1.84	1.09	147.7	0.586	0.414	3.45	4.9

X_s and X_{agg}, weight fractions of single chains and aggregates, respectively; $M_{w,agg}$, molecular weight of the aggregates; N_{agg}, aggregation number.
[a] Values of the parameters in the concentration range CAC $< C < C^*$.

$M_{w,agg}$, as well as the weight fractions of the single chains and the aggregates, X_s and X_{agg}, respectively. The combination of static and dynamic light scattering has been used to estimate the above parameters [36–40]. The basic principle is outlined elsewhere [39] and leads to Eq. (8):

$$M_w^*/X_s = M_{w,s} + M_{w,s}/A_r \quad (8)$$

where $M_{w,s}$ is the weight-average molecular weight determined in the concentration range well below CAC (Table 2), M_w^* is the apparent weight-average molecular weight averaged over the double distribution of the single coils and aggregates determined in the concentration range CAC $< C < C^*$ (Table 3). The only unknown parameters are X_s and the area ratio, A_r. Here A_r is defined as

$$A_r = A_s A_{agg} \quad (9)$$

where A_s and A_{agg} are the peak areas from DLS of the single coils and aggregates, respectively. A_r was determined by extrapolation of A_s/A_{agg} to zero angle (Fig. 10a) and then by extrapolation of $(A_{agg}/A_s)_{q=0}$ to zero concentration (Fig. 10b).

After knowing A_r, X_s was calculated from Eq. (8); X_{agg} was easily obtained from $X_{agg} = 1 - X_s$. The values of X_s and X_{agg} are summarized in Table 3. On the other hand, for M_w^* that contains contribution from both individual chains and aggregates one can write (Eq. (10))

$$M_w^* = M_{w,s}X_s + M_{w,agg}X_{agg} \quad (10)$$

Here, the unknown parameter $M_{w,agg}$ was calculated and the values are listed in Table 3. The aggregation numbers, N_{agg}, calculated from Eq. (11)

$$N_{agg} = M_{w,agg}/M_{w,s} \quad (11)$$

are also given in Table 3. The resulting N_{agg} values varied from 2.5 to 4.9 chains per particle. Such low values of the aggregation number were expected; the scaling law describing the molecular weight dependence of the aggregation number is given by Eq. (12)

$$N_{agg} \sim m^{-\nu} \quad (12)$$

where m is the number of monomer units in the corona-forming block. This simply means that N_{agg} is lower at a higher m-value. The theoretically predicted [41] and experimentally found [42,43] values of ν for EO-based copolymers are 0.51 and 0.6, respectively. Limitations of sample availability, however, prevented us from verifying the validity of the described above scaling law for our copolymers.

Another parameter that can be extracted from the data is the average extension of the coronal chains. The latter was calculated according to Eq. (13).

$$\%\text{extension} = (\delta/am)100 \quad (13)$$

where $\delta = R_h^{agg} - R_{core}$ is the corona thickness and $a = 0.35$ nm is the length of one oxyethylene unit. In these calculations the core radius, R_{core}, could be neglected since the corona thickness constitutes the greater part of the aggregate radius. This assumption leads to slight overestimation of the values of the percentage of coronal extension. The latter were found to be very low (2.5–3.1%) implying that the coronae were much less extended compared to those of starlike micelles [44–48]. This finding is consistent with the low aggregation number and the extremely long coronal chains.

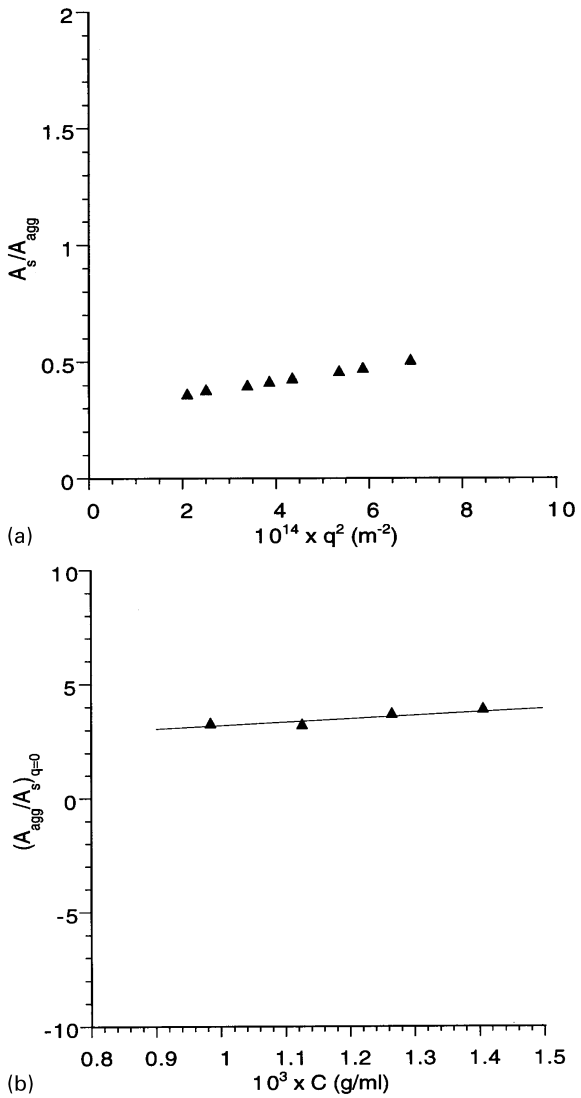

Fig. 10. (a) Angular dependence of the area ratio of the single coil and aggregate peaks for the copolymer PEO-Brij76GE at 0.984×10^{-3} g/ml. (b) Concentration dependence of the extrapolated to zero angle area ratio.

Based on the results and the data analysis the following picture of the coronae can be deduced. Due to their large dimensions and extremely high molecular weights the PEO chains in the coronae are in close contact and thus are highly entangled. They are much less extended compared to the coronal chains of lower molecular weight materials. The proposed model is depicted in Fig. 11.

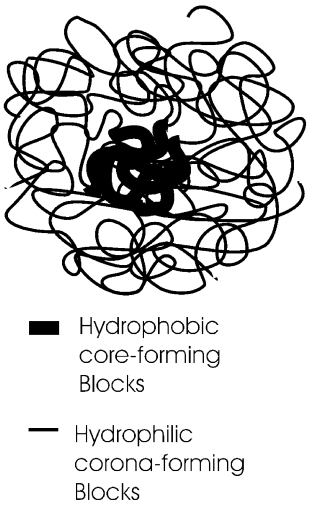

Fig. 11. Schematic representation of the aggregates with hydrophobic alkylglycidyl ether core and hydrophilic PEO corona.

The relatively compact conformation is stabilized by intra- and intermolecular hydrogen bonding, mediated by water molecules. In this respect the coronae are quite similar to the microgel, which has been demonstrated to form in HMW PEO of molecular weights above 6×10^5 [10].

3.4. Transmission electron microscopy

TEM micrographs showed that the copolymers formed separated particles from diluted aqueous solutions (Fig. 12).

The dimensions of the particles are in the 30–60 nm range—somewhat smaller than those determined by LS. The difference can be attributed with the corona shrinkage due to dehydration during the drying process by the sample preparation. Remarkable is fact that even at these hydrophilic/hydrophobic ratios the particles are spherical—a form typical for the majority of amphiphilic block copolymers in diluted solutions at ambient temperature. Concerning the behaviors of amphiphiles in aqueous solutions, we suppose core-corona morphology for nanoparticles obtained. Furthermore, as can be clearly seen on the micrographs, some of the objects (dark domains) are surrounded by a halo of weaker contrast, which can be attributed to the long PEO chains forming the particles coronae.

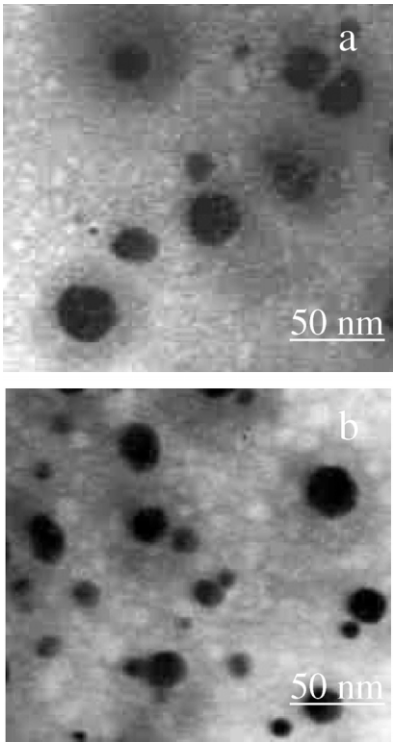

Fig. 12. Transmission electron micrographs of diblock copolymers: PEO-Brij72GE (a), and PEO-Brij76GE (b).

4. Conclusion

Core-corona nanoparticles were prepared from novel high molecular weight amphiphilic poly(ethylene oxide)-*b*-poly(alkylglycidyl ether) diblock copolymers, in which the hydrophobic aliphatic groups were separated from the main chain by flexible oxyethylene spacers. Copolymers of such unique structure and high molecular weight were used for the first time to prepare PEO-based polymeric nanoparticles.

At low concentrations the copolymers behaved as unmodified high molecular weight homo PEO in aqueous solution, i.e. they were only slightly affected by the presence of the hydrophobic blocks. By increasing the concentration the copolymers were found to self-associate. The aggregation process occurred in a relatively narrow concentration range and critical aggregation concentrations of about 1.1×10^{-3} g/ml were determined by fluorescence. The aggregates were characterized by low aggregation numbers (3–5) and a core-corona morphology, as revealed from the LS and the TEM micrographs, respectively. The PEO chains in the coronae were in close contact and highly entangled, which resulted in the formation of less extended coronae compared to the coronae of lower molecular weight amphiphilic copolymers. In analogy to high molecular weight homo PEO, it is anticipated that the compact conformation is stabilized by intra- and intermolecular hydrogen bonding. Hence, the present nanoparticles display markedly different features from those of the core-corona particles formed by amphiphilic materials of lower molecular weights, and thus are characterized by an enhanced aggregate stability.

Acknowledgements

The synthesis of the block copolymers was performed in 1997–1998 as a part of research project supported by Union Carbide Corporation, Bound Brook. The authors express their gratitude to Dr Alan Theis and Dr Jonatan Leder

(UCC, Bound Brook) for helpful discussions. S.R. thanks the Swedish Technical Research Council for providing a grant supporting his stay in Sweden.

References

[1] Torchilin VP. J Controlled Release 2001;73:137.
[2] Jones M-C, Leroux J-C. Eur J Pharm Biopharm 1999;48:101.
[3] Allen C, Maysinger D, Eisenberg A. Colloids Surf, B: Biointerf 1999; 16:3.
[4] Kwon GS, Okano T. Adv Drug Delivery Rev 1996;21:107.
[5] Cho C-S, Nah J-W, Jeong Y-I, Cheon J-B, Asayama S, Ise H, Akaike T. Polymer 1999;40:6769.
[6] Fendler JH. Chem Mater 1996;8:1616.
[7] Munk P, Prochazka K, Tuzar Z, Webber SE. Chemtech 1998;20.
[8] Wu C, Liu T, Chu B, Schneider DK, Graziano V. Macromolecules 1997;30:4574.
[9] Harada A, Kataoka K. J Controlled Release 2001;72:85.
[10] Rangelov S, Brown W. Polymer 2000;41:4825.
[11] Novakov Ch, Vladimirov N, Stamenova R, Tsvetanov ChB. Macromol Symp 2000;161:169.
[12] Hasan E, Jankova K, Samichkov V, Ivanov Y, Tsvetanov ChB. Macromol Symp 2002;177:125.
[13] Dimitrov Ph, Hasan E, Rangelov S, Trzebicka B, Dworak A, Tsvetanov ChB. Polymer, in press.
[14] Rangelov S, Petrova E, Berlinova I, Tsvetanov ChB. Polymer 2001; 42:4483.
[15] Munk P, Rangelov S, Tuzar Z. Int J Polym Anal Charact 1998;4:435.
[16] Rangelov S, Tuzar Z. J Mater Sci Lett 1999;18:221.
[17] Almgren M, Brown W, Hvidt S. Colloid Polym Sci 1995;273:2.
[18] Alami E, Almgren M, Brown W. Macromolecules 1996;29:2229.
[19] Rangelov S, Almgren M, Tsvetanov Ch, Edwards K. Macromolecules 2002;35:4770.
[20] Panayotov IM, Berlinova IV, Bojilova M, Boyadjiev A, Rachkov IB, Tsvetanov Ch. Bulgarian Patent 25,142;1978.
[21] Tsvetanov ChB, Dimitrov I, Doytcheva M, Petrova E, Dotcheva D, Stamenova R. In: Quirk RP, editor. Applications of anionic polymerization research. ACS Symposium Series 696. Washington, DC: ACS; 1996. p. 236.
[22] Peracchia MT, Desmaele D, Couvreur P, díAngelo J. Macromolecules 1997;30:846.
[23] Tanford C, Nozaki Y, Rohde MF. J Phys Chem 1977;81:1555.
[24] Kalyanasundaram K, Thomas JK. J Am Chem Soc 1977;99:2039.
[25] Zana R. In: Zana R, editor. Surfactant solutions: new methods of investigation. Sutfactant science series 22, New York: Marcel Dekker; 1987. p. 241.
[26] Chu DY, Thomas JK. In: Rabek JF, editor. Photochemistry and photophysics, vol. 3. Boca Raton, FL: CRC Press; 1991. p. p. 49.
[27] Dong DC, Winnik MA. Can J Chem 1984;62:2560.
[28] Petit-Agnely F, Iliopoulos I, Zana R. Langmuir 2000;16:9921.
[29] Liu F, Frere Y, Francois J. Polymer 2001;42:2969.
[30] Devanand K, Selser JC. Nature 1990;343:978.
[31] Porsch B, Sundelof L-O. Macromolecules 1995;28:7165.
[32] Cotts PM, Selser JC. Macromolecules 1990;23:2050.
[33] Devanand K, Selser JC. Macromolecules 1991;24:5943.
[34] Benmouna M, Akcasu AZ. Macromolecules 1980;13:409.
[35] de Gennes PG. Scaling concepts in polymer physics. Ithaca, NY: Cornell University Press; 1979.
[36] Wu C, Mohammad S, Woo KF. Macromolecules 1995;28:4914.
[37] Kirill NB, Iwao T, William JM, Frank EK. Macromolecules 1993;26: 1972.
[38] Zhou Z, Peiffer DG, Chu B. Macromolecules 1994;27:1428.
[39] Zhang Y, Wu C, Fang Q, Zhang Y-X. Macromolecules 1996;29:2494.
[40] Seery T, Yassini M, Hogen-Esch T, Amis E. Macromolecules 1992; 25:4784.
[41] Nagarajan R, Ganesh K. J Chem Phys 1989;90:5843.
[42] Booth C, Attwood D. Macromol Rapid Commun 2000;21:501.
[43] Chainbundit C, Mai S-M, Heatley F, Booth C. Langmuir 2000;16: 9645.
[44] Moffitt M, Yu Y, Nguyen D, Graziano V, Schneider DK, Eisenberg A. Macromolecules 1998;31:2190.
[45] Yang Y-W, Yang Z, Zhou Z-K, Attwood D, Booth C. Macromolecules 1996;29:670.
[46] Zhou Z, Chu B. Macromolecules 1994;27:2025.
[47] Kabanov AV, Nazarova IR, Astafieva IV, Batrakova EV, Alakhov VY, Yaroslavov AA, Kabanov VA. Macromolecules 1995;28:2303.
[48] Chu B. Langmuir 1995;11:414.